

AD-A195 821

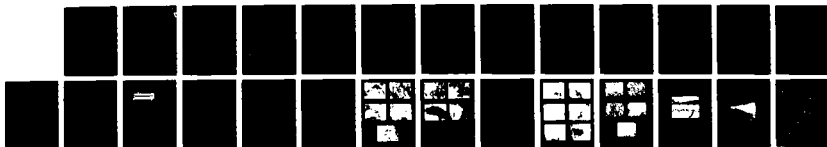
MORPHOLOGICAL CHANGES IN POLYMER ELECTROLYTE CELLS (U)
MINNESOTA UNIV MINNEAPOLIS CORROSION RESEARCH CENTER
H 2 MUNSHI ET AL. MAY 88 ONR-TR-18

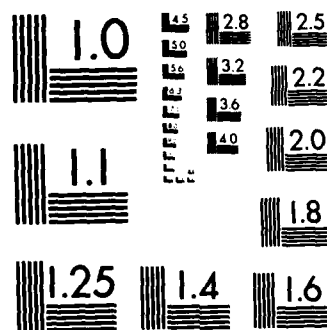
1/1

UNCLASSIFIED

F/G 10/3

ML





MICROCOPY RESOLUTION TEST CHART
NATIONAL BUREAU OF STANDARDS-1963-A

OTIC FILE COPY

SECURITY CLASSIFICATION OF THIS PAGE

4

REPORT DOCUMENTATION PAGE

AD-A195 821

2b. DECLASSIFICATION / DOWNGRADING SCHEDULE

1b. RESTRICTIVE MARKINGS

3. DISTRIBUTION / AVAILABILITY OF REPORT

Unclassified/Unlimited

JUN 30 1988

4. PERFORMING ORGANIZATION REPORT NUMBER(S)

5. MONITORING ORGANIZATION REPORT NUMBER(S)

ONR Technical Report 18

6a. NAME OF PERFORMING ORGANIZATION

6b. OFFICE SYMBOL (If applicable)

7a. NAME OF MONITORING ORGANIZATION

Corrosion Research Center

Office of Naval Research, Resident Rep.

6c. ADDRESS (City, State, and ZIP Code)

University of Minnesota
Minneapolis, MN 55455

7b. ADDRESS (City, State, and ZIP Code)

Federal Building, Room 286
536 South Clark Street
Chicago, IL 60605-1588

8a. NAME OF FUNDING / SPONSORING ORGANIZATION

8b. OFFICE SYMBOL (If applicable)

9. PROCUREMENT INSTRUMENT IDENTIFICATION NUMBER

Office of Naval Research

Code 1113

Contract No. N00014-85-1588

6c. ADDRESS (City, State, and ZIP Code)

810 North Quincy Street
Arlington, VA 22217-5000

10. SOURCE OF FUNDING NUMBERS

PROGRAM
ELEMENT NO.

PROJECT
NO.

TASK
NO.

WORK UNIT
ACCESSION NO.

11. TITLE (Include Security Classification)

Morphological Changes in Polymer Electrolyte Cells

12. PERSONAL AUTHOR(S)

M.Z.A. Munshi, & B.B. Owens

13a. TYPE OF REPORT

Technical

13b. TIME COVERED

FROM 7/15/85 TO 5/30/88

14. DATE OF REPORT (Year, Month, Day)

May 1988

15. PAGE COUNT

23

16. SUPPLEMENTARY NOTATION

Accepted for publication in Solid State Ionics, June 1988

17. COSATI CODES

FIELD

GROUP

SUB-GROUP

18. SUBJECT TERMS (Continue on reverse if necessary and identify by block number)

polymer electrolytes, morphology, lithium, cells, *May 1988*

19. ABSTRACT (Continue on reverse if necessary and identify by block number)

Rechargeable solid state batteries utilizing lithium anodes, V_6O_{13} composite cathodes and polymer electrolytes made from polyethylene oxide - $LiCF_3SO_3$ complex were investigated at 100°C. The cells exhibited good cycling and reversibility. Optical and scanning electron microscopy were used the morphological changes taking place at the electrodes and electrolyte as a function of cycle number. Post-mortem examination of the cell material indicated that the structures of lithium, electrolyte and cathode become finer grained and hence smoother. In addition the structures were more coherent. The cathode appeared to undergo a re-healing process during the early stage of cycling. The results indicate that the structures are consistent with one another and that long cycle life can be obtained with these types of cells.

Keyman

20. DISTRIBUTION / AVAILABILITY OF ABSTRACT

☒ UNCLASSIFIED/UNLIMITED ☐ SAME AS RPT ☐ OTIC USERS

21. ABSTRACT SECURITY CLASSIFICATION

Unclassified

22a. NAME OF RESPONSIBLE INDIVIDUAL

Boone B. Owens

22b. TELEPHONE (Include Area Code)

(612) 625-1332

22c. OFFICE SYMBOL

Morphological Changes in
Polymer Electrolyte Cells

M.Z.A. Munshi
B.B. Owens

Department of Chemical Engineering and Materials Science
Corrosion Research Center
University of Minnesota
221 Church St. SE
Minneapolis, MN 55455

ABSTRACT

Rechargeable solid state batteries utilizing lithium anodes, V_6O_{13} composite cathodes and polymer electrolytes made from polyethylene oxide - $LiCF_3SO_3$ complex were investigated at 100°C. The cells exhibited good cycling and reversibility. Optical and scanning electron microscopy were used to study the morphological changes taking place at the electrodes and electrolyte as a function of cycle number. Post-mortem examination of the cell material indicated that the structures of lithium, electrolyte and cathode become finer grained and hence smoother. In addition the structures were more coherent. The cathode appeared to undergo a re-healing process during the early stage of cycling. The results indicate that the structures are consistent with one another and that long cycle life can be obtained with these types of cells.

Accession For	
NTIS GRA&I	<input checked="checked" type="checkbox"/>
DTIC TAB	<input checked="checked" type="checkbox"/>
Unannounced	<input type="checkbox"/>
Justification	
By	
Distribution/	
Availability Codes	
Dist	Avail and/or Special
A-1	



1. INTRODUCTION

The discovery of ionically conducting polymers by Fenton and co-workers [1] followed by Armand's [2] proposal for an all-solid-state battery have had a strong impact worldwide on solid state battery research. Since then a large number of groups have investigated a variety of polymer electrolytes such as polyethylene oxide (PEO) complexes of various lithium salts [3-7]. The feasibility of these polymer electrolyte batteries has been tested in a variety of research cells and in some prototype hardware of practical size [8-10]. Nevertheless there are at present no commercially available polymer electrolyte batteries. Most of the emphasis has been directed towards secondary batteries utilizing lithium anodes and intercalation cathodes such as TiS_2 or V_6O_{13} .

In this communication a detailed study presents the effect of cycling on the morphology of the lithium, electrolyte and composite V_6O_{13} cathode elements in solid state cells operating at 100°C . Both optical and scanning electron microscopy were employed. Until recently, studies of this kind [11] were made largely on cycled TiS_2 cathodes. However, there is no available literature that describes the morphological changes taking place within the electrode phases during cell cycling. One factor is that these solid state polymer electrolyte systems are fairly new and long-term cycling and failure effects have yet to be reported. This paper records a study of the electrodes and electrolyte surfaces which provides photographic results complementary to the cycling data.

2. EXPERIMENTAL

2.1 Preparation of the Cell Material

The handling and fabrication of the cell materials were carried out as described elsewhere [12].

2.2 Cell Construction and Cycling

Cells were assembled in the dry room as shown in Figure 1. The geometrical surface area of the electrolyte, cathode and lithium was effectively 6.4 cm^2 . Polypropylene spacers were used to separate the two electrodes. Two layers of electrolyte were employed in each cell. Each cell was sandwiched between two stainless steel plate current collectors and a clamping system was used to maintain a constant pressure and electrode gap. The cells were cycled in an oven at 100°C in the glove box.

The theoretical capacity of the cathode was based on 8 Li insertion into the V_6O_{13} structure. The electrode loading was about 1.8 to 2 mAhcm^{-2} . In all cases a constant current discharge and a constant voltage charge through a limiting resistor were employed. In this study the microscopic examination was conducted on cells discharged at the C/5 rate.

2.3 Microscopy

All cells were examined in the discharged state. After the requisite number of cycles had been completed, the cells were removed from the oven and cooled to

room temperature. They were opened in the dry room atmosphere. Each electrode and electrolyte sample were carefully peeled from one another to obtain a clean examinable surface. In some cases this was not possible so only cross-sections were examined.

Optical micrographs were obtained using an Olympus SZ III optical microscope equipped with a polaroid camera.

Scanning electron micrographs were obtained using a JEOL 840II scanning electron microscope. An accelerating voltage of 20 kV was used in order to avoid charging of the sample as well as beam damage. Despite this the lithium samples were found to be experiencing beam damage from the electron gun.

Cathode samples containing predominantly $\text{Li}_x\text{V}_6\text{O}_{13}$ and carbon were sufficiently electrically conductive so that no electrostatic charging of the samples by the electron beam was experienced. On the other hand samples containing large quantities of electrically insulating PEO electrolyte could be observed directly only at low magnifications because of charging effects. However, the resolution was not too good because of the low accelerating voltage. Somewhat better resolution was obtained with the electrolyte cross-section if the cathode layer was also intact. Because of these limitations, only the cathode was studied in sufficient detail by SEM.

3. RESULTS AND DISCUSSION

3.1 Cycling

The initial open-circuit voltage of the cells at room temperature was over 3.5V. However, at 100°C, this value stabilized to 2.9-3.1V.

Figure 2 shows typical families of discharge curves for a 13 mAh cell at various rates from the 40h (C/40) rate to the 1h (C) rate, operating at a temperature of 100°C [10]. The cut-off voltage was +1.8V. The discharge curves have several distinct plateaus and these are thought to be characteristic of the change in the oxidation state of the V_6O_{13} cathode. Another factor that may give rise to these plateaus is the apparent continuous increase in the IR drop of the cell during discharge [12]. It is believed that this increase originates not only from changes taking place at the cathode, but also due to a change in the electrolyte resistivity as a result of counter ion transport to the anode. During recharge there is a loss in capacity compared to the initial discharge.

A plot of the theoretical capacity versus the number of cycles is shown in Figure 3 [12]. At low rates, the initial capacity is considerably greater than at high rates, as expected. However, the decline in capacity is much faster at the lower rates of discharge than at the higher rate, with greater stabilization in capacity occurring at the C/5 rate. These results are consistent with the work of Hooper and North [8]. At the C/5 rate, a hundred cycles were obtained with greater than 75% of the initial utilization of V_6O_{13} being maintained at cycle number 100. From cycle number 35 to cycle number 100 the coulombic efficiency was almost 100% with very little reduction in the capacity.

3.2 Microscopic Examination

Post-mortem examination of the cell using optical microscopy showed the anode-electrolyte-cathode interfaces to be well intact.

Figures 4a-e are optical micrographs (magnification of 50x) of the lithium surface at the interface with the electrolyte. Figure 4a shows a typical optical micrograph of the fresh lithium surface. The surface appears to be bounded by "planes" in a random orientation with no evidence of lithium particulates. After the first discharge, (Figure 4b) the number of "planes" increases somewhat. At cycle number 10, the frequency of occurrence of these "planes" increases considerably. Continued cycling changes the surface further (Figure 4d). Finally after 100 cycles (Figure 4e), the structure is more dimpled. By comparing the micrographs of Figures 4a and 4e, the structure has become finer grained and hence smoother. The development of very little individual lithium particle growth is fairly obvious. The dramatic change during cycling is clearly the result of continuous electro-oxidation and electro-reduction of the lithium. Furthermore there is no evidence of dendrites in any of these micrographs. Instead, cycling appears to aid in producing a uniform lithium surface.

Figure 5a-d are optical micrographs of the electrolyte surface at the interface with the cathode. Because of its weakly reflecting nature, fresh samples of the PEO electrolytes could not be resolved well by optical microscopy. However, after cycle number 2 (Figure 5a), the electrolyte surface appears to have a fluffy structure. The darker spots are from the cathode. The mottled appearance is quite evident and these are caused by the cathode particulate

structure. After cycle number 10 (Figure 5b), the mottling components disappear with the emergence of a more uniform structure. At this stage the electrolyte has a cloudy appearance. At cycle number 35, (Figure 5c), the electrolyte appears to be more translucent and somewhat crystalline. Figure 5d shows the surface structure after cycle number 100. A comparison with the micrograph of Figure 5a shows that there is an important difference between the early state of the electrolyte and that surface produced at cycle number 100. A complete transformation appears to take place during cycling. Again the surface has a dimpled-like appearance, tending towards more homogeneity and uniformity compared to the previous micrographs.

It must be remembered that the samples are surface structures photographed at the interface with the cathode and so only a two-dimensional effect is given. Nonetheless, some three-dimensional crystals of the electrolyte are clearly evident in the micrograph of Figure 5d (bottom left-hand corner). It is interesting to note, however, that these well-defined interior electrolyte crystals are occluded by a continuous uniform layer of the surface electrolyte with no evidence of surface cracks.

A detailed examination of the cathode was made not only using optical but also scanning electron microscopy because of the better resolution and higher magnification possible with the latter technique.

Figures 6a-f show the corresponding optical micrographs of the cathode surfaces interfaced with the electrolyte. Figure 6a is the cathode after the casting process. The surface layer is fairly reflective (due to surface PEO) and

highly smooth with large numbers of streak marks traversing in one plane only. These are probably caused by the casting process. Figure 6b shows a micrograph of the cathode having undergone 10% depth of discharge of the first cycle. The structure is remarkably different from the initial state. Numerous cracks of 50-100 μ m in width are clearly evident with the surface considerably less intact compared to the original cathode. After 40% depth of discharge of the first cycle, (Figure 6c), the cracks become less frequent, (widths about 100-250 μ m) and instead a re-healing process occurs. The surface also appear more intact, porous and grainy, as can be seen from the deposit on the white aluminum current collector. At the end of cycle number 5, (Figure 6d) the cracks almost disappear. The re-healing process is further exemplified in this micrograph by the faint light markings on the surface. Only a few striations are evident with the cathode now beginning to take a uniform shape.

After cycle number 35, the cracks are non-existent and the surface appears extremely porous, smooth and homogeneous. In addition, the grainier structure is apparent. At cycle number 100, (Figure 6f), these grains become even finer, such that the porous structure is now absent. The surface structure is even more smooth and uniform. The remarkable changes occurring between cycles number 5 and 100 are clearly evident. The optical micrographs suggest that the cathode undergoes a re-healing process between cycle number 0 and cycle number 5. This could be compared to the "forming" process of porous electrodes in conventional batteries. Once "formed," the material tends to become more coherent and highly smooth.

It is interesting to note that the crystalline electrolyte deposits

mentioned earlier are much more visible in Figure 6f.

A series of scanning electron micrographs were obtained of the cathode at 1000x (Figure 7a-e). A micrograph of the cast cathode was not possible because of severe charging arising from the PEO electrolyte. However Figure 7a shows a micrograph of a cathode after completing cycle number 1. The surface appears fairly well intact and careful examination suggests the particles are fused to one another. This is probably due to the PEO acting as a binder. These areas can be readily distinguished as lighter shades. This is actually the result of charging by the PEO.

A clearer look at these fibrous materials can be seen from a cross-section of the sample, shown in Figure 7a. Figure 8 provides a better view of such fibers including the well-defined structure of V_6O_{13} and carbon particulates fused by the PEO electrolyte. However these fused structures tend to be less resolvable with further cycling.

Figure 7b depicts a micrograph after the fifth discharge. The particles are now more segregated with little evidence of charging. The size of the particles range from 2-10 μm .

After 35 cycles, (Figure 7c), the material becomes finer grained with an average grain size of $< 2\mu\text{m}$. The particles are well-defined and the surface appears more porous. After cycle number 100, the grains are so small that they could not be resolved at 1000x (Figure 7d). A micrograph taken at 5000x shows the cathode to be extremely porous with grain size in the sub-micron range. The

white patches in both micrographs may well be the PEO electrolyte. A comparison of Figures 7a through 7e graphically demonstrates the morphological changes with cycling.

Figure 9 shows a cross-section of the cell after cycle number 5 showing the lithium, electrolyte, cathode and aluminum backing. The cell exhibits good adhesion at the anode/electrolyte and electrolyte/cathode interfaces, even after 100 deep cycles.

The above results suggest that the structures of the lithium, electrolyte and cathode are consistent with one another and with the cycling data. The study vividly demonstrates that during cycling, the cell material structure actually improves. If this is so, the cell should give several hundred cycles without appreciable degradation of the electrolyte or the active materials. This is evident to some extent in the cell cycled 100 times. After cycle number 34, the capacity decrease is almost negligible.

4. CONCLUSION

The difference between the morphology of the surface structures of the individual cell components after the initial and subsequent electrochemical cycles in solid state cells of the type $\text{Li} | (\text{PEO})_8 \cdot \text{LiCF}_3\text{SO}_3 | \text{V}_6\text{O}_{13}$ is evident. The unique fine grained character of the surface obtained by a continuous cycling process is of considerable importance in the development process for the interfacial regions.

ACKNOWLEDGEMENT

This work was supported in part by the Office of Naval Research.

REFERENCES

1. B.E. Fenton, J.M. Parker, and P.V. Wright, *Polymer*, 14, 589, (1973).
2. M. Armand, J.M. Chabagno and M. Duclot, in "Fast Ion Transport in Solids," (eds. P. Vashista, J.N. Mundy and G.K. Shenoy) North-Holland, Amsterdam, 131, (1979).
3. J.M. North, C.A.C. Sequeira, A. Hooper and B.C. Tofield, 1st Int. Meeting on Li Batteries, Abs. # 32, Rome, Italy (1982).
4. A. Hooper, in "Solid State Batteries," (eds. C.A.C. Sequeira and A. Hooper), NATO. ASI Series, Martinus Nijhoff Publishers, 399, (1985).
5. C.D. Robitaille and D. Fauteux, *J. Electrochem. Soc.* 133(2), 315, (1986).
6. J.E. Weston and B.C.H. Steele, *Solid State Ionics*, 2, 347, (1981).
7. M. Minier, C. Berthier and W. Gorecki, *ibid*, 9/10, 1125, (1983).
8. A. Hooper and J.M. North, *ibid*, 9/10, 1161, (1983).
9. M. Gauthier, D. Fauteux, G. Vassort, A. Belanger, M. Duval, P. Ricoux, J.M. Chabagno, D. Muller, P. Rigaud, M.B. Armand and D. Deroo, *J. Electrochem. Soc.* 132, 1333, (1985).
10. M.Z.A. Munshi and B.B. Owens, 172nd Meeting of the Electrochem. Soc., Abs. #83, Honolulu, Hawaii, Oct. 18-23, (1987).
11. M. Gauthier, lecture presented at Florida Atlantic University Short Course on Li Batteries, (Mar. 1987)
12. M.Z.A. Munshi and B.B. Owens, *Solid State Ionics*, 1, 46, (1988).

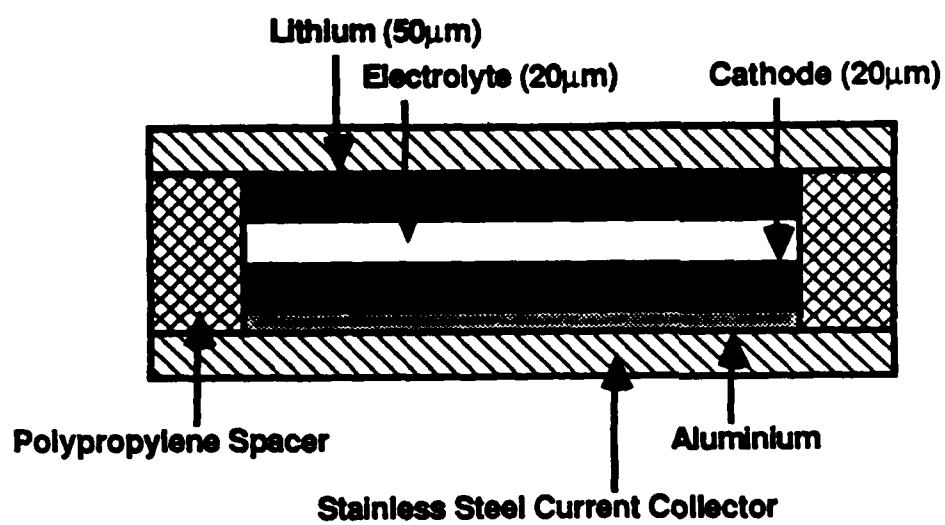


Figure 1. Schematic of the polymer electrolyte cell.

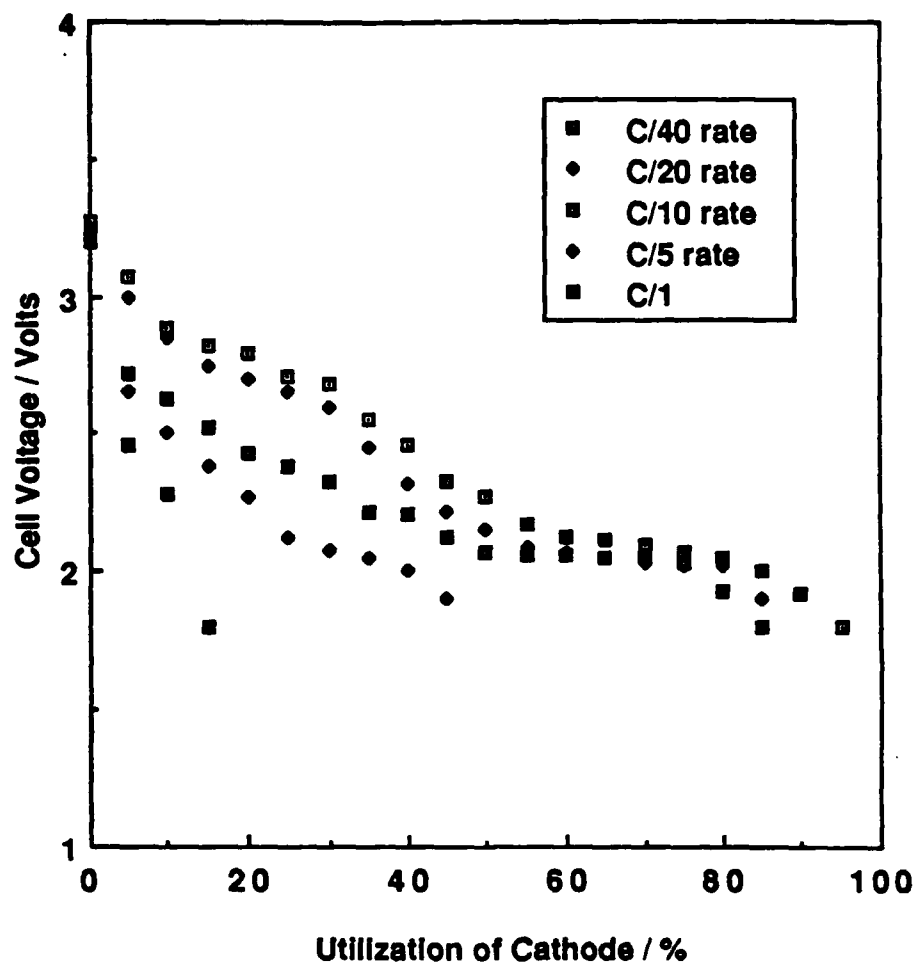


Figure 2. Typical family of discharge curves at 100°C.

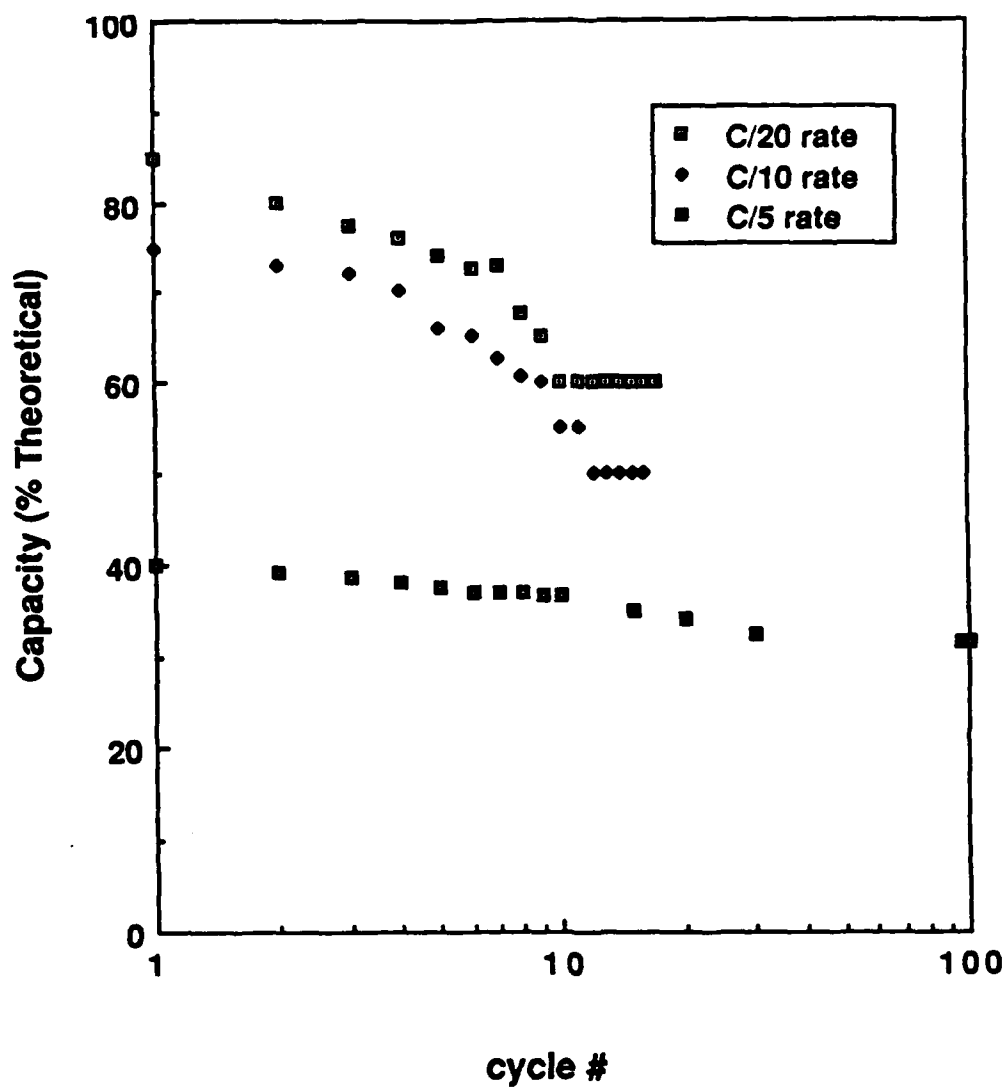


Figure 3. Plot of capacity versus cycle # for cells at 100°C.

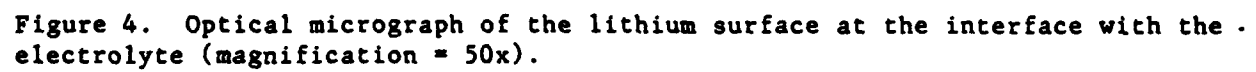
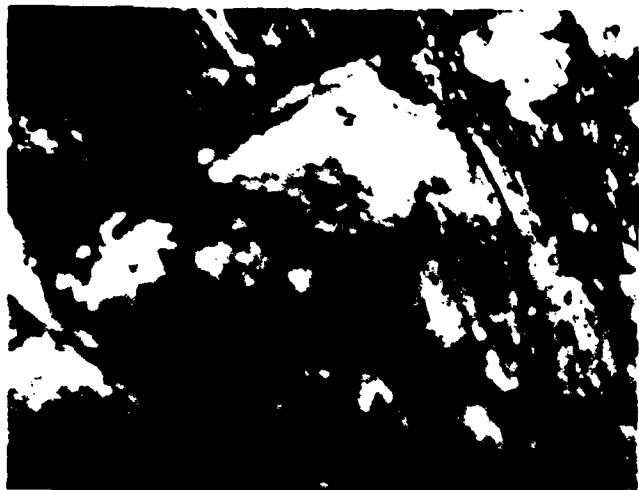
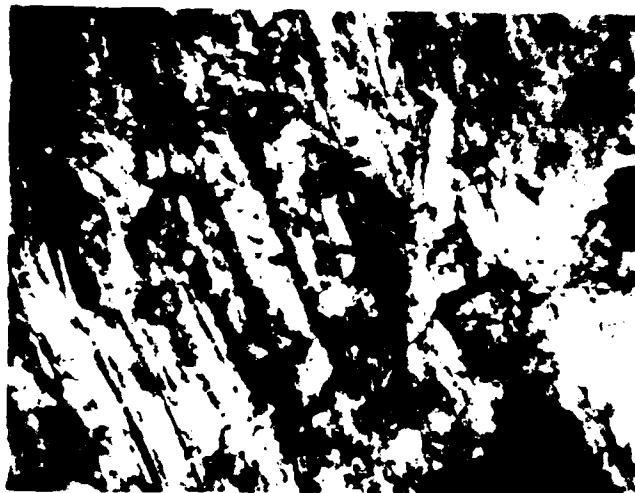
The image is a black and white optical micrograph showing a lithium surface at its interface with an electrolyte. The surface appears relatively smooth but with some subtle texture and variations in tone, suggesting a microscopic view of the material's surface. The interface is clearly defined by the change in the surface's appearance.

Figure 4. Optical micrograph of the lithium surface at the interface with the .
electrolyte (magnification = 50x).



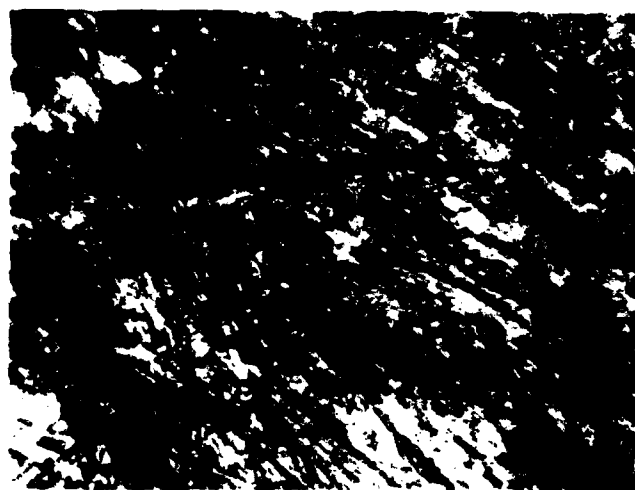
(a) Cycle # 0



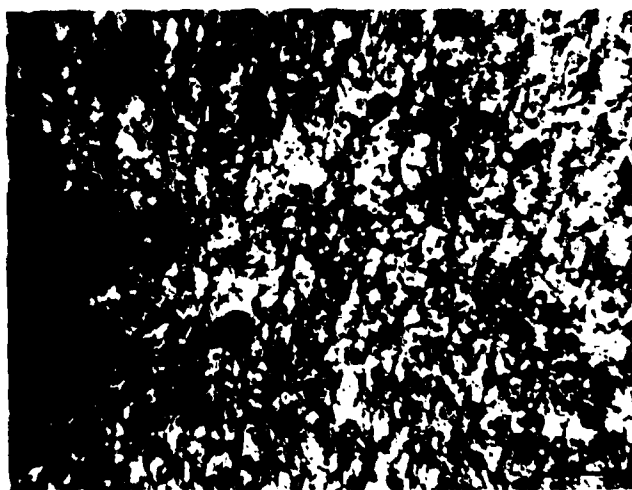
(b) Cycle # 1



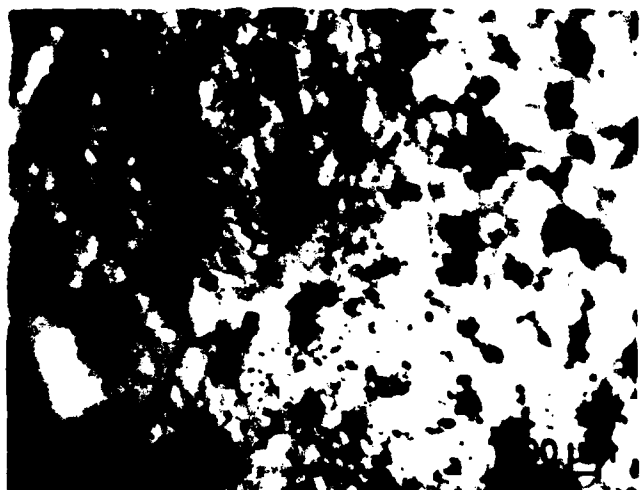
(c) Cycle # 10



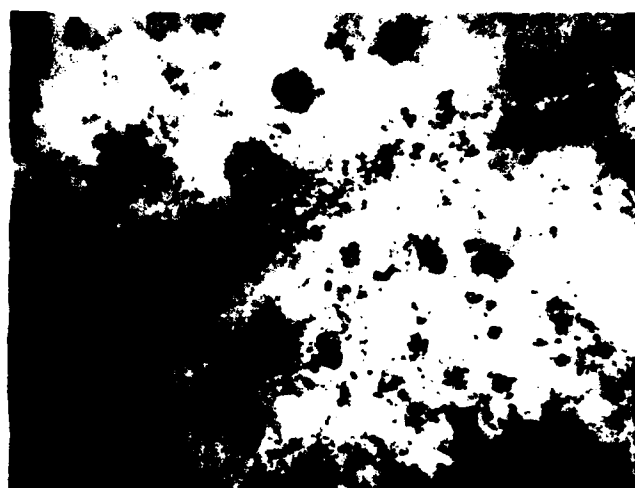
(d) Cycle # 35



(e) Cycle # 100



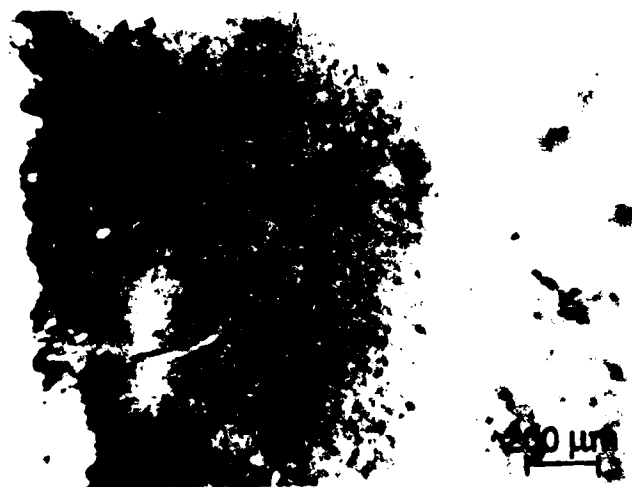
(a) Cycle # 2



(b) Cycle # 10



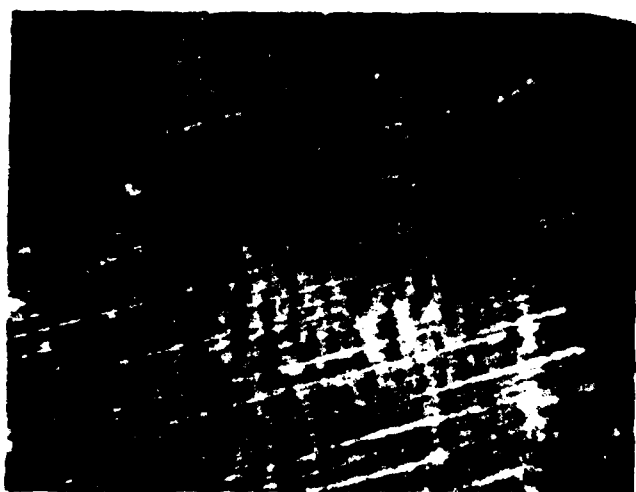
(c) Cycle # 35



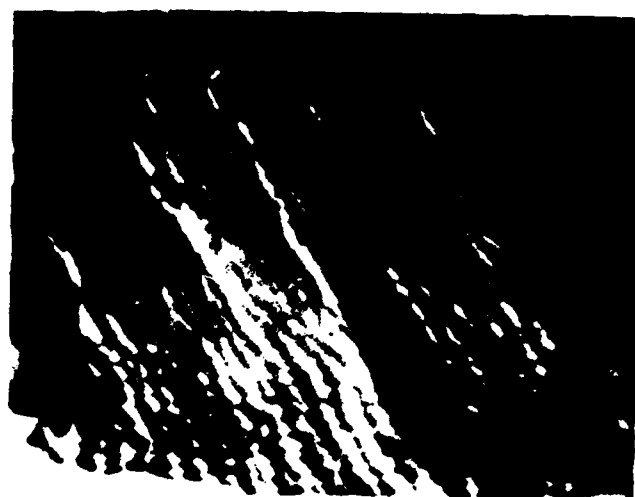
(d) Cycle # 100

Figure 5. Optical micrograph of the electrolyte surface at the initial and final stages of magnification = 50x

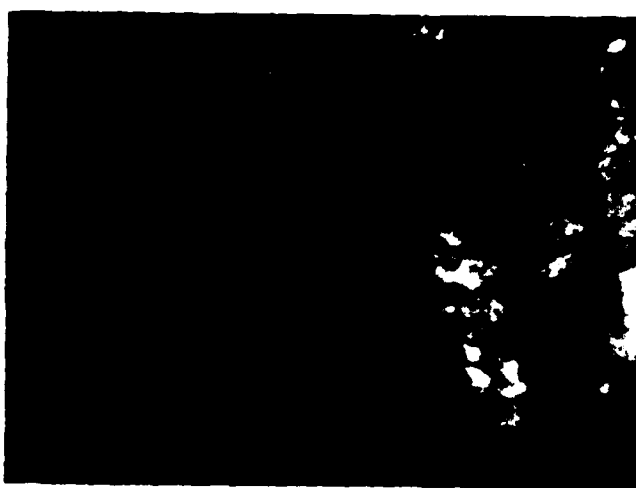
Figure 6. Optical micrograph of the cathode surface at the interface with the electrolyte (magnification = 50x).



(a) Cycle # 0



(b) 10% Discharge



(c) 40% Discharge



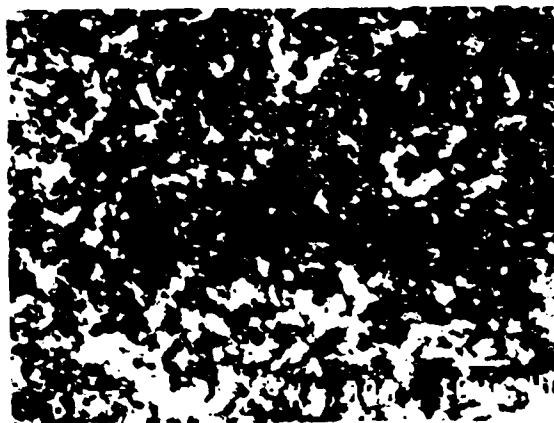
(d) Cycle # 5



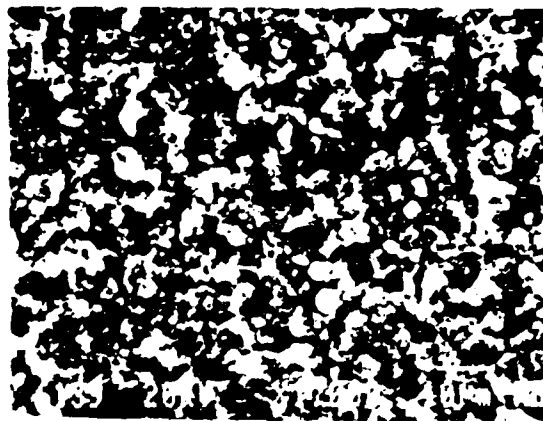
(e) Cycle # 35



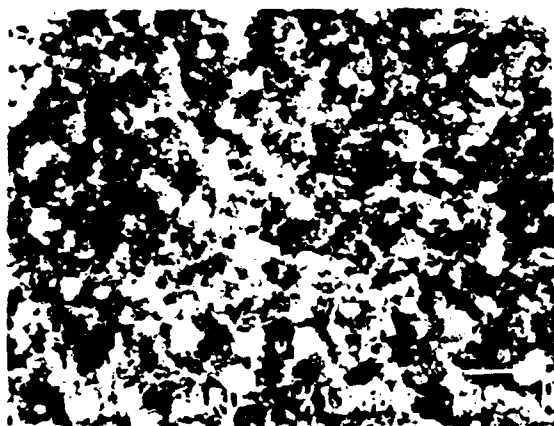
(f) Cycle # 100



(a) cycle #1



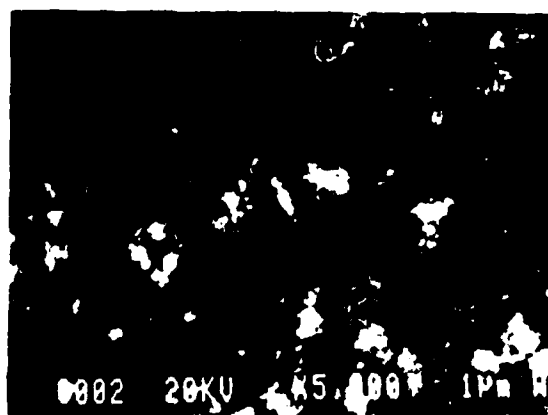
(b) cycle #5



(c) cycle #35



(e) cycle #100



(d) cycle #100

Figure 7 SEM photographs of cycled cathodes

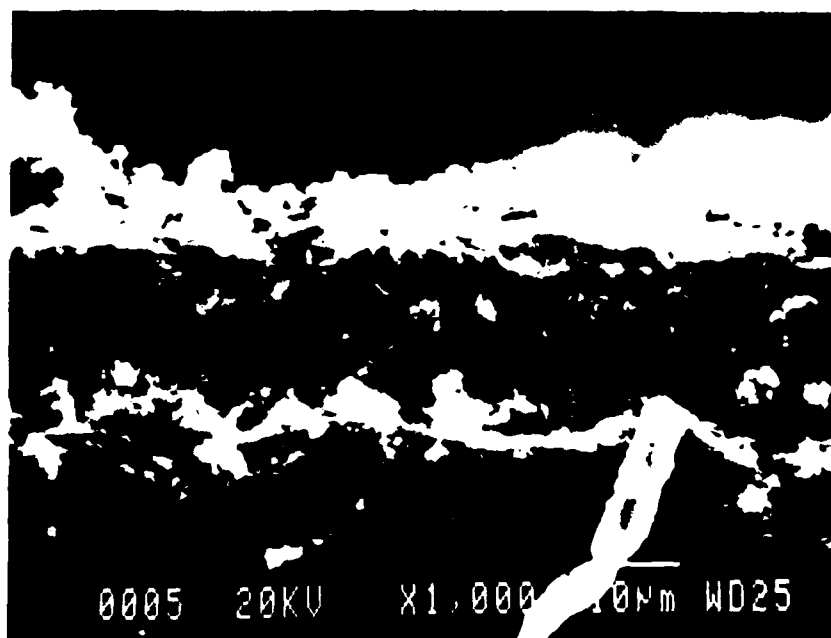


Figure 8. Scanning electron micrograph of the electrolyte cross-section

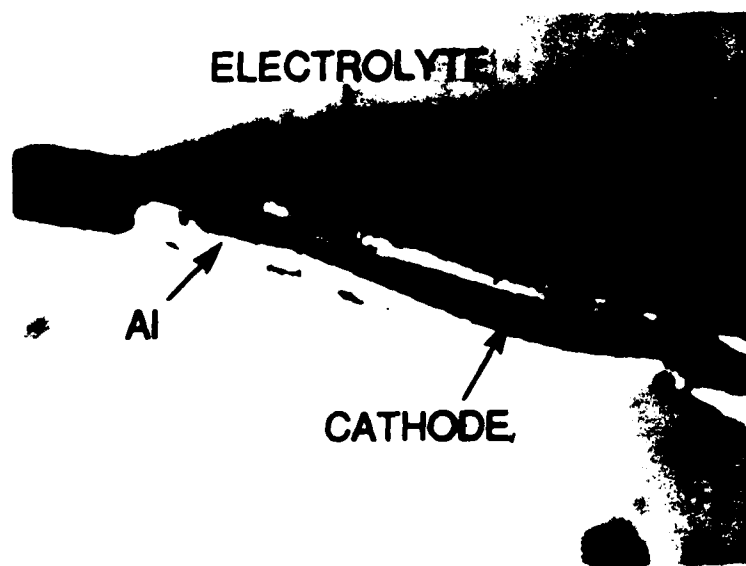


Figure 9. Cross-sectional view of a cell after cycle #5

END

DATE

FILMED

9-88

DTIC